

## Symmetry determination following structure solution in *P1*

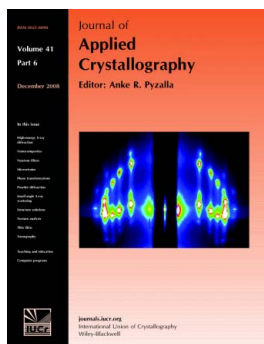
L. Palatinus and A. van der Lee

*J. Appl. Cryst.* (2008). **41**, 975–984

Copyright © International Union of Crystallography

Author(s) of this paper may load this reprint on their own web site or institutional repository provided that this cover page is retained. Republication of this article or its storage in electronic databases other than as specified above is not permitted without prior permission in writing from the IUCr.

For further information see <http://journals.iucr.org/services/authorrights.html>



Many research topics in condensed matter research, materials science and the life sciences make use of crystallographic methods to study crystalline and non-crystalline matter with neutrons, X-rays and electrons. Articles published in the *Journal of Applied Crystallography* focus on these methods and their use in identifying structural and diffusion-controlled phase transformations, structure–property relationships, structural changes of defects, interfaces and surfaces, *etc.* Developments of instrumentation and crystallographic apparatus, theory and interpretation, numerical analysis and other related subjects are also covered. The journal is the primary place where crystallographic computer program information is published.

Crystallography Journals **Online** is available from [journals.iucr.org](http://journals.iucr.org)

# Symmetry determination following structure solution in *P1*

L. Palatinus<sup>a\*</sup> and A. van der Lee<sup>b</sup>Received 10 June 2008  
Accepted 3 September 2008

<sup>a</sup>Laboratoire de Cristallographie, Le Cubotron, Ecole Polytechnique Fédérale de Lausanne, 1015 Lausanne, Switzerland, and <sup>b</sup>Institut Européen des Membranes, UMR-CNRS 5635, Université Montpellier II, Place Eugène Bataillon, cc 047, 34095 Montpellier Cedex 5, France. Correspondence e-mail: lukas.palatinus@epfl.ch

A new method for space-group determination is described. It is based on a symmetry analysis of the structure-factor phases resulting from a structure solution in space group *P1*. The output of the symmetry analysis is a list of all symmetry operations compatible with the lattice. Each symmetry operation is assigned a symmetry agreement factor that is used to select the symmetry operations that are the elements of the space group of the structure. On the basis of the list of the selected operations the complete space group of the structure is constructed. The method is independent of the number of dimensions, and can also be used in solution of aperiodic structures. A number of cases are described where this method is particularly advantageous compared with the traditional symmetry analysis.

© 2008 International Union of Crystallography  
Printed in Singapore – all rights reserved

## 1. Introduction

The determination of the correct space-group symmetry is one of the steps in the complete structural analysis of a crystalline material by diffraction techniques. Usually different methods are combined in order to reduce the number of different space groups that are compatible with the experimental data; firstly the experimental Laue symmetry of the intensity-weighted reciprocal lattice reduces the number of possible space groups to those of the Laue class. Secondly the existence or non-existence of so-called systematic absences for certain reflection classes betrays the presence or absence of nonsymmorphic symmetry operations. The combination of the different systematic absences leads to the construction of the extinction symbol; combined with the correct Laue symmetry the diffraction symbol is obtained. The *International Tables for Crystallography* (Hahn, 2002) can be used to look up to which possible space group a certain diffraction symbol corresponds. Only in 50 cases does a diffraction symbol uniquely define a space group; in all other cases between two and five different possibilities exist for the correct space group. A further reduction of the possibilities can be made by considering the ratio of the average observed intensity for specific classes of reflections over that of general reflections to indicate the presence of different nonsymmorphic symmetry elements. Alternatively, space-group frequency tables based on the occurrence of space groups in databases such as the Cambridge Structural Database (CSD) for organic and organo-metallic compounds, the Inorganic Crystal Structure Database (ICSD) for inorganic compounds, and the Protein Data Bank (PDB) for protein structures are used to discriminate between the different possibilities. The statistics of

properly normalized structure factors can be used to discriminate between centrosymmetric and noncentrosymmetric space groups with the same diffraction symbol. The space group selected by the combination of these methods is subsequently used for the structure-solution step and validated by a successful structure refinement.

Although in the majority of cases the determination of the correct space group is relatively straightforward, problematic cases can hamper structure solution occasionally. There are different reasons why the standard methods may fail; especially in the case of weak data it may be difficult to discriminate between 'observed' and 'non-observed' reflections, so that the presence of nonsymmorphic symmetry operations may easily be overlooked. This is also the case if the data are strong but a result of the presence of, for example, stacking faults in the structure or if the Renninger effect diffraction intensity is observed for 'forbidden' reflections. The methods that are based on statistics have the obvious drawback that they only give a certain probability for the correct choice. In powder diffraction the correct choice of the space group is nearly always problematic, because of the overlap of reflection peaks. Several advanced space-group determination methods have been proposed for powder data, all being probabilistic in nature (Markvardsen *et al.*, 2001; Altomare *et al.*, 2004). For incommensurate structures only *JANA2006* (Petříček *et al.*, 2006) has an option to guide the choice of the space group based on an analysis of systematic extinction conditions. The difficulties here are that satellite reflections are in general rather weak, so that it is often difficult to decide between 'observed' and 'non-observed' reflection classes. Another problem is that the range of the satellite index is usually very small (1–4) so that the number of reflections on which the

analysis is based is also very small, making the assessment of what is extinct and non-extinct statistically not very reliable.

The difficulty in determination of the space group arises from the simple fact that the space-group determination precedes the structure solution. This is necessary if the knowledge of the symmetry is used in the structure-solution process. However, it has been mentioned several times in the past that in some cases direct methods perform better if the solution is attempted in *P1* (Sheldrick & Gould, 1995; Burla *et al.*, 2000). Moreover, recently, powerful structure-solution methods have appeared that make no use of the symmetry for structure solution at all (Oszlányi & Sütő, 2004, 2007; Elser, 2003). In all such cases the symmetry determination can be performed after the structure solution.

On the basis of the idea that the determination of the symmetry from the phased structure factors is principally an easier task than if only diffracted intensities are used, we propose here a novel method for determining the correct space-group symmetry. It relies on a symmetry analysis of the phase set resulting from the structure solution in *P1*. It can find in one step symmorphic and nonsymmorphic symmetry operations, and detects as well the presence or absence of inversion centers. It is noted that the algorithm was developed for a program *SUPERFLIP* (Palatinus & Chapuis, 2007) where it is used to determine the symmetry in a scattering density obtained by the charge-flipping algorithm (Oszlányi & Sütő, 2004), and charge flipping is thus the structure-solution method used in this study. However, the method can be used with any structure-solution method solving a higher-symmetrical structure in *P1*. The new space-group determination method can also be used for aperiodic structures described in a  $(3+d)D$ -dimensional space.

Interestingly a method for locating the *known* space-group symmetry in a scattering density has been devised several times in the past in different contexts (Hendrixson & Jacobson, 1997; Burla *et al.*, 2000; Palatinus, 2004), but to our knowledge nobody has made the step towards reconstructing the complete space group without any *a priori* assumptions.

We first outline in detail the symmetry-searching procedure before presenting a number of examples that illustrate the method. The method is compared with a number of other space-group determination methods.

## 2. Symmetry determination in electron-density maps

In this section we present an algorithm for an automatic detection of the most probable space group of a crystal structure represented by its scattering density. The input to the symmetry-searching algorithm is a scattering density  $\rho$  in one unit cell, or, equivalently, a list of phased structure factors obtained by a Fourier transform of the scattering density.  $\rho$  is typically an electron density, but it can also be a neutron scattering density or a potential density; positivity is not required. It is further assumed that the scattering density represents a structure solution in *P1*, *i.e.* without any assumptions on its symmetry. As a result, the true symmetry of the structure is present in the scattering density only

approximately, and the origin of the space group is randomly positioned in the unit cell.

The algorithm can be decomposed into the following steps:

- (i) Determine the lattice centering
- (ii) Generate the complete list of possible symmetry operations compatible with the lattice
- (iii) Assign a figure of merit to each symmetry operation, and select the symmetry operations that belong to the space group of the structure
- (iv) Complete and validate the space group
- (v) Shift the position of the symmetry operations to a conventional origin

Conceptually the algorithm is not complicated, but each step can be implemented in several ways differing in details. What follows is a description of the algorithm, as it is implemented in the computer program *SUPERFLIP*. *SUPERFLIP* has been from the beginning designed to work in arbitrary dimensions in order to allow also for structure solution of two-dimensional structures, modulated structures and quasicrystals. Therefore, the symmetry-searching algorithm, as it is described here, does not rely in any manner on the dimensionality of the analyzed scattering density.

### 2.1. Lattice centering

Determination of the lattice centering must be the first step of the symmetry determination for reasons to become clear in §2.5. The easiest way to determine the lattice centering is to analyze the autocorrelation function (Patterson function)  $P = \rho(\mathbf{r}) \star \rho(-\mathbf{r})$ . If  $\rho(\mathbf{r}) = \rho(\mathbf{r} + \mathbf{v})$ , *i.e.* if  $\rho$  exactly contains a nonzero centering vector  $\mathbf{v}$ , then  $P$  will have a maximum at  $\mathbf{v}$  with a height equal to the origin peak. If the centering is only approximate, the peak will be lower than the origin peak. Once the candidates for a centering vector are found in the Patterson function, we use the following value to evaluate the significance of each candidate:

$$R(\mathbf{v}) = \frac{\sum_{\mathbf{h}, \mathbf{h}+\mathbf{v}=\text{integ.}} |F(\mathbf{h})|^2}{\sum_{\mathbf{h}} |F(\mathbf{h})|^2}, \quad (1)$$

where the summation runs over all the structure factors calculated from  $\rho$ . The value of  $R(\mathbf{v})$  depends only on the amplitudes and not on the phases of the structure factors and as such can be determined prior to the structure solution. In practice the centering is often determined already at the data-reduction stage, and very often the reflections extinct as a result of the lattice centering are not included in the final data set at all. Therefore we decided to set a relatively strict acceptance limit for the centering vector. The vector  $\mathbf{v}$  is accepted as a centering vector of the space group if  $R(\mathbf{v}) > 0.98$ , which means that the sum of intensities of the reflections extinct because of the centering must be less than 2% of the total sum of intensities. Setting a more relaxed limit would increase the tolerance to the noise in the data, but at the cost of accepting a false centering vector in cases of superstructures, where the differences between individual subcells are often very small.

Using the Patterson function for detection of the lattice centering is essentially equivalent to a search for systematic absences, but it does not require a table of possible reflection classes to test, and therefore detects also nonstandard centering vectors and is applicable to structures in any dimension.

## 2.2. List of symmetry operations

The second step in the symmetry determination is a derivation of all the symmetry operations that are compatible with the lattice parameters and lattice centering. A necessary and sufficient condition for a matrix  $\mathbf{R}$  to represent a rotational part of potential symmetry operation  $\mathcal{S} = \{\mathbf{R}|\boldsymbol{\tau}\}$  is

$$\mathbf{R}^T \mathbf{G} = \mathbf{G} \mathbf{R}^{-1}, \quad (2)$$

where the superscript T denotes the transpose of the matrix and  $\mathbf{G}$  is the metric tensor  $g_{ij} = \mathbf{a}_i \cdot \mathbf{a}_j$ .<sup>1</sup>  $\mathbf{R}$  is an integer matrix, and, if the lattice basis is symmetry adapted, then  $\mathbf{R}$  contains only 0,  $-1$  and 1. If the search for possible rotation matrices is not limited to matrices with elements 0,  $-1$  and 1, then the algorithm will be able to detect symmetry even in a non-canonical basis, for example, a hexagonal symmetry in a structure described in a monoclinic basis. However, allowing matrices with elements larger than 1 results in an increased list of possible symmetry operations. In practice it is unlikely that a higher-symmetrical lattice basis will be missed thanks to the advanced algorithms in most of the data-reduction software. Therefore, for the sake of saving computational time, the search in *SUPERFLIP* is currently limited to matrices with elements 0,  $-1$  and 1.

Each potential rotational part  $\mathbf{R}$  compatible with equation (2) must be combined with all possible translation vectors  $\boldsymbol{\tau}$  to obtain complete symmetry operations. Because the position of the symmetry element in the unit cell is to be determined later and can be arbitrary, it makes sense to derive only the intrinsic translation vectors  $\boldsymbol{\tau}^{\text{int}}$ . These vectors fulfill the equation

$$k\boldsymbol{\Omega}\boldsymbol{\tau}^{\text{int}} = k\boldsymbol{\tau}^{\text{int}} = \boldsymbol{\nu} \text{ mod integer}, \quad (3)$$

where  $k$  is the order of  $\mathbf{R}$ ,  $\boldsymbol{\nu}$  is any lattice-centering vector including the zero vector and  $\boldsymbol{\Omega}$  is the projection operator:  $\boldsymbol{\Omega} = (1/k) \sum_{i=1}^k \mathbf{R}^i$ . Using equation (3) it is an easy task to generate a complete list of possible intrinsic translation vectors  $\boldsymbol{\tau}^{\text{int}}$  for each of the potential rotational parts  $\mathbf{R}$ . As a result, a complete list of symmetry operations  $\mathcal{S} = \{\mathbf{R}|\boldsymbol{\tau}^{\text{int}}\}$  compatible with the lattice is obtained.

## 2.3. Finding the origin-dependent translation vector of a symmetry operation

The method for determination of the position of a symmetry element in the unit cell has been described in detail elsewhere (Hendrixson & Jacobson, 1997; Palatinus & Chapuis, 2007), but let us briefly review it here, adapted for the present purpose. Let us assume that  $\rho$  is approximately

<sup>1</sup> For an introduction and discussion of the concepts used throughout this section, such as metric tensors, intrinsic translation, projection operators *etc.*, see Hahn (2002), especially ch. 8 by H. Wondratschek.

symmetrical according to a symmetry operation  $\mathcal{S} = \{\mathbf{R}|\boldsymbol{\tau}\}$ .  $\boldsymbol{\tau}$  can be located as a maximum in the correlation function  $C(\mathbf{d})$  between  $\rho$  and its image transformed by  $\mathbf{R}$ :

$$C(\mathbf{d}) = \int \rho(\mathbf{r}) \rho(\mathbf{R}\mathbf{r} + \mathbf{d}) \text{d}\mathbf{r}. \quad (4)$$

The translational part  $\boldsymbol{\tau}$  has intrinsic and origin-dependent components:  $\boldsymbol{\tau} = \boldsymbol{\tau}^{\text{int}} + \boldsymbol{\tau}^{\text{or}}$ . Several symmetry operations can have the same rotational part  $\mathbf{R}$  but different intrinsic translational parts, and therefore it is not enough to locate the absolute maximum of  $C(\mathbf{d})$ , because in such a case the translational part of only one of the whole family of symmetry operations would be determined. To obtain the optimal position of a symmetry operation with rotational part  $\mathbf{R}$  and intrinsic translational part  $\boldsymbol{\tau}^{\text{int}}$ , the maximum value of  $C(\mathbf{d})$  must be searched only at such points  $\mathbf{d}$ , where  $\mathbf{d} - \boldsymbol{\tau}^{\text{int}}$  is a purely origin-dependent translation vector for matrix  $\mathbf{R}$ , *i.e.*  $\boldsymbol{\Omega}\mathbf{d} = \boldsymbol{\tau}^{\text{int}}$ .

## 2.4. Determination of the symmetry operations compatible with the scattering density

This stage is the essential part of the symmetry-searching algorithm. It is necessary to evaluate each potential symmetry operation and decide if it belongs to the space group of the structure or not. If  $\rho$  is perfectly symmetrical according to  $\mathcal{S} = \{\mathbf{R}|\boldsymbol{\tau}\}$ , then the following relation between structure factors is valid:

$$F_{\mathbf{h}} = F_{\mathbf{h}\mathbf{R}} \exp(2\pi i \mathbf{h}\boldsymbol{\tau}). \quad (5)$$

Thus, the phase difference between  $F_{\mathbf{h}}$  and  $F_{\mathbf{h}\mathbf{R}}$  can be used to estimate how well the symmetry operation  $\mathcal{S}$  is present in  $\rho$ . The phase difference for reflection  $\mathbf{h}$  and that related by  $\mathcal{S}$  can be defined as

$$\Delta_{\mathbf{h},\mathcal{S}} = |\varphi(\mathbf{h}) - \varphi(\mathbf{h}\mathbf{R}) - 2\pi \mathbf{h} \cdot \boldsymbol{\tau} + 2\pi n|, \quad (6)$$

where  $\varphi$  denotes the phase of the structure factor and  $n$  is an integer number such that  $\Delta_{\mathbf{h},\mathcal{S}}$  has the smallest value. There are many ways to combine  $\Delta_{\mathbf{h},\mathcal{S}}$  of all reflections into a single figure of merit, the most obvious being a simple average or mean phase difference. Another possibility is to use directly the value of  $C(\mathbf{d})$ . Burla *et al.* (2000) propose another criterion (called S2), which is closely related to the value of  $C(\mathbf{d})$ . All these criteria have in common that they are linear or close to linear in at least a part of the interval of  $\Delta_{\mathbf{h},\mathcal{S}}$ . However, our tests show that criteria involving the first power of  $\Delta_{\mathbf{h},\mathcal{S}}$  are prone to noise, and it is not easy to find a quantitative limit between a good and a bad value. Using a higher power of  $\Delta_{\mathbf{h},\mathcal{S}}$  appears more favorable in this respect, and therefore we chose the following criterion, a weighted mean-square phase difference, which we call the symmetry agreement factor  $\phi_{\text{sym}}$ :

$$\phi_{\text{sym}}(\mathcal{S}) = C \frac{\sum_{\mathbf{h}} |F_{\mathbf{h}} F_{\mathbf{h}\mathbf{R}}|^2 \Delta_{\mathbf{h},\mathcal{S}}^2}{\sum_{\mathbf{h}} |F_{\mathbf{h}} F_{\mathbf{h}\mathbf{R}}|}. \quad (7)$$

The normalization constant  $C = 3/\pi^2$  is selected so that a completely random density will give  $\phi_{\text{sym}} = 1$ . A perfectly symmetrical density will, of course, result in  $\phi_{\text{sym}} = 0$ .  $\phi_{\text{sym}}(\mathcal{S})$

must be calculated for every potential symmetry operation  $\mathcal{S}$  from the list. All operations with  $\phi_{\text{sym}}(\mathcal{S})$  below a certain threshold are then considered to be elements of the space group of the structure. The acceptance threshold is the second and last parameter of the algorithm (the first being the threshold for acceptance of the centering vector). Its value strongly depends on the method used for the structure solution and on the quality of the data. If the method is charge flipping or another dual-space iterative structure-solution method, the data quality is good, and proper steps are undertaken to improve the solution after the convergence (Palatinus & Chapis, 2007; Oszlányi & Sütő, 2008), then according to our experience  $\phi_{\text{sym}}$  for the correct symmetry operations is most frequently below 0.1, and almost always below 0.2, while  $\phi_{\text{sym}}$  for the wrong symmetry operations is usually above 0.5. In *SUPERFLIP* the default acceptance threshold is 0.25, and this limit works very well in a vast majority of cases, although it can fail occasionally in cases of very noisy data, especially data extracted from powder patterns or data from a twinned crystal.

### 2.5. Completing and validating the space group

At this stage we have produced a list of symmetry operations that are most likely the elements of the space group of the structure. The main goal of the algorithm is completed, and, indeed, often the list of symmetry operations with their  $\phi_{\text{sym}}$  suffices and the crystallographer can immediately judge the correct space group. However, to make the space-group determination completely automatic, the space group must also be automatically validated and completed. In an ideal case the list of accepted symmetry operations contains all the elements of the space group and nothing else. In practice this is most often the case. However, two mechanisms can break this ideal situation. Firstly, if the quality of the data or solution is low, some of the true symmetry elements can have  $\phi_{\text{sym}}$  above the acceptance threshold. In such a case it is necessary to generate the missing operations to complete the space group. Secondly, in the case of pseudosymmetry false symmetry operations can occur with  $\phi_{\text{sym}}$  only slightly above the  $\phi_{\text{sym}}$  of the correct operations. A general case of pseudosymmetry cannot be easily detected, but a specific type of pseudosymmetry occurs if the structure consists of multiple copies of a smaller subcell with small deviations between the subcells. These cases are characteristic of pseudotranslations relating the subcells of the true cell. In such cases pairs of symmetry operations can exist, whose combination results in such a pseudotranslation. It is thus advisable to eliminate the symmetry operations that, if combined with other operations with smaller  $\phi_{\text{sym}}$ , result in a nonprimitive translation other than the known centering vectors. It is for this reason that it was necessary to determine the centering vectors in advance (§2.1). This procedure is especially important for modulated structures with weak modulations, where such pseudotranslations along the additional dimensions are more a rule than an exception.

With the above considerations in mind, the space-group completion is quite straightforward. The procedure is initiated by sorting the symmetry operations by ascending  $\phi_{\text{sym}}$  and by forming a trivial space group with one element – the identity. Then one element at a time is taken from the sorted list and added to the list of elements of the space group. This augmented list of elements is then completed to form again a space group by combining the new element with all other space-group elements. If any of the newly generated symmetry operations is a false nonprimitive translation, then all the symmetry operations added to the space group based on the last element are discarded. This procedure is repeated with all symmetry operations in the list with  $\phi_{\text{sym}}$  below the acceptance threshold.

### 2.6. Shifting the origin

The output of the procedure described in the preceding sections is a complete space group of the structure, and the task of finding the space group is essentially completed. However, the space group still has an arbitrary origin, and it is convenient to shift the origin to a more conventional one. Hahn (2002) defines conventional origins for all two- and three-dimensional space groups, but in general there is no unambiguous choice of origin of a space group. Thus, a computer program implementing the algorithm can either resort to a table of space groups to find the conventional origin or use an algorithm to locate an origin using a small number of explicit rules, which, however, is not guaranteed to be the conventional one. For higher-dimensional space groups only the second possibility is applicable, since no conventional origins exist for dimensions higher than three. In any case this issue is only a minor problem, because the position of the origin is not essential for the description of the structure, and most modern crystallographic programs can deal with space-group settings with nonconventional origin.

## 3. Examples

### 3.1. Weak data

Weak data often thwart the determination of the space group based on the analysis of systematic extinctions, since the distinction between reflections with observable intensity [with *e.g.*  $I > 3\sigma(I)$ ] and those systematically absent [and thus necessarily  $I < 3\sigma(I)$ ] becomes less clear. From our experience it was observed that problems of this nature start to arise when the mean value of the ratio of the intensity and its estimated standard deviation for a given resolution,  $\langle I/\sigma(I) \rangle$ , drops below 10. The example in this section concerns a structure flo19, an organic molecule,  $\text{C}_{62}\text{H}_{46}\text{N}_{14}$ ,  $Z = 1$ , that crystallizes in a primitive orthorhombic space group with two short and one very long axis, giving diffraction data with  $\langle I/\sigma(I) \rangle = 6.81$ . The analysis of the relevant systematic absences is summarized in Table 1.

The systematic absences suggest  $P-2_12_1/n$  as diffraction symbol, but this is a non-existing symbol in Laue class *mmm* [ $R_{\text{int}}(\text{mmm}) = 0.06$ ]. Taking possible combinations of the

**Table 1**  
Systematic absences for crystal flo19†.

The column '*t/f*' gives the ratio of columns 3 and 4. The column 'True' for  $\phi_{\text{sym}}$  indicates the symmetry agreement for the nonsymmorphic symmetry element corresponding to the fulfilled reflection condition, and the column 'False' that for the corresponding symmorphic symmetry element.  $\phi_{\text{sym}} = 0.72$  for the inversion center. Bold values indicate  $\phi_{\text{sym}}$  lower than 0.25.

Class	Condition	$\langle I/\sigma(I) \rangle$		No. of reflections		<i>t/f</i>	$\phi_{\text{sym}}$	
		True	False	True	False		True	False
<i>h00</i>	$h = 2n$	1.84	0.35	3	5	5.23	<b>0.09</b>	0.41
<i>0k0</i>	$k = 2n$	52.20	5.69	2	2	9.18	0.40	<b>0.10</b>
<i>00l</i>	$l = 2n$	8.93	1.04	41	43	8.61	<b>0.04</b>	0.88
<i>0kl</i>	$l = 2n$	8.04	5.73	428	428	1.40	0.99	0.61
<i>0kl</i>	$k = 2n$	6.19	7.68	458	398	0.81	1.32	0.61
<i>0kl</i>	$k + l = 2n$	7.20	6.57	426	430	1.10	0.92	0.61
<i>h0l</i>	$l = 2n$	8.92	8.15	230	231	1.09	0.75	0.80
<i>h0l</i>	$h = 2n$	6.05	10.50	204	257	0.58	1.22	0.80
<i>h0l</i>	$h + l = 2n$	9.27	7.81	229	232	1.19	0.67	0.80
<i>hk0</i>	$k = 2n$	4.72	16.24	41	38	0.29	0.81	0.70
<i>hk0</i>	$h = 2n$	5.43	13.91	34	45	0.39	0.91	0.70
<i>hk0</i>	$h + k = 2n$	19.49	1.71	38	41	11.43	0.72	0.70

† Cell parameters:  $a = 3.91, b = 6.17, c = 51.22 \text{ \AA}, \alpha = 90, \beta = 90, \gamma = 90^\circ, V = 1236.4 \text{ \AA}^3, \langle I/\sigma(I) \rangle = 6.81$  for all data.

**Table 2**  
Squared structure-factor amplitudes for *hk0* reflections.

<i>hkl</i>	$ F _{\text{meas}}^2$	$ F _{\text{calc}}^2$	$\sigma( F _{\text{meas}}^2)$	<i>hkl</i>	$ F _{\text{meas}}^2$	$ F _{\text{calc}}^2$	$\sigma( F _{\text{meas}}^2)$
200	462.72	321.36	146.48	210	500.43	365.23	98.41
110	74943.42	77477.83	349.31	310	450.69	499.72	157.19
020	110818.00	110601.12	1084.62	120	37.73	24.56	250.69
220	1731.50	1684.83	116.41	320	1892.20	2045.95	168.87
130	4679.84	3748.31	133.46	030	3040.15	2542.88	278.63
330	1253.49	1297.54	261.51	230	184.02	87.63	116.20
040	729.12	363.94	328.70	140	143.34	69.77	126.21
240	242.35	215.45	185.16	050	189.41	112.32	411.52
150	95.48	241.93	528.03	250	234.98	54.57	554.50

symmetry elements either  $P--n$  or  $P-2_12_1$  can thus be proposed as possible diffraction symbol. It appears, however, that it is impossible to solve the structure with the direct method programs *SIR2004* (Burla *et al.*, 2005) and *SHELXS* or *SHELXD* (Sheldrick, 2008) starting from the space groups compatible with the diffraction symbols, *viz.*  $Pm\bar{m}n, Pm2_1n, P2_1mn$  and  $P22_12_1$ . The structure solution with *SUPERFLIP* proceeds smoothly, since the structure is solved in  $P1$ ; intensities were averaged according to Laue symmetry  $mmm$  and subsequently expanded to  $P1$ . No *a priori* assumptions were made concerning systematic absences, *i.e.* all reflections were included in the data set. The subsequent symmetry analysis shows that the correct space group is actually  $P2_122_1$ , which is confirmed by the structural refinement that follows. A control using *PLATON*'s *ADDSYM* option (Spek, 2003) does not show any additional symmetry. Interestingly, the  $n^c$ -glide, which clearly shows up in the list of systematic absences, is absent in the final structure with a symmetry agreement factor of only 0.72. An inspection of the refined structure shows that in the projection of the structure onto the *ab* plane a large part of the atoms are related by the centering vector  $(\frac{1}{2}, \frac{1}{2})$ , which in combination with the generally low intensities leads to the pseudoextinction effect in the *hk0* plane. It is now interesting

**Table 3**  
Systematic absences for crystal flo2†.

Class	Condition	$\langle I/\sigma(I) \rangle$		No. of reflections		<i>t/f</i>
		True	False	True	False	
<i>0k0</i>	$k = 2n$	32.20	14.74	12	13	2.18
<i>00l</i>	$l = 2n$	39.53	13.04	37	37	3.03
<i>00l</i>	$l = 4n$	78.35	9.55	18	56	8.20
<i>0kl</i>	$l = 2n$	20.67	22.11	1525	1516	0.93
<i>0kl</i>	$k = 2n$	36.30	7.41	1471	1570	4.90
<i>0kl</i>	$k + l = 2n$	20.73	22.05	1525	1516	0.94
<i>hk0</i>	$h + k = 2n$	30.77	26.28	228	226	1.17
<i>hhl</i>	$l = 2n$	20.12	21.29	1032	1038	0.95

† Cell parameters:  $a = 19.12, b = 19.12, c = 43.3 \text{ \AA}, \alpha = 90, \beta = 90, \gamma = 90^\circ, V = 15829 \text{ \AA}^3, \langle I/\sigma(I) \rangle = 15.36$  for all data.  $\phi_{\text{sym}} = \mathbf{0.08}$  ( $4_1^c$ ); **0.13** ( $2_1^c$ ); 0.68 ( $4^c$ ); 0.70 ( $1$ ); 0.76 ( $2^{a-b}$ ); 0.79 ( $m^c$ ); 0.80 ( $b^a$ ); 0.82 ( $m^a$ ); 0.86 ( $2_1^a$ ); 0.86 ( $m^{a+b}$ ); 0.87 ( $2^c$ ); 0.88 ( $4^c$ ); 0.88 ( $n^{a-b}$ ); 0.90 ( $n^c$ ); 0.90 ( $2^a$ ); 0.97 ( $n^a$ ); 1.04 ( $c^a$ ). Bold values indicate  $\phi_{\text{sym}}$  lower than 0.25.

to compare the calculated *hk0* squared structure factors resulting from the final refinement using the structural model without the  $n^c$ -glide with the observed squared structure factors that suggested the presence of an  $n^c$ -glide. Table 2 shows that the reflections *hk0*:  $h + k = 2n + 1$  are indeed correctly calculated. A detailed description of the structure will be published elsewhere (Dimutru *et al.*, 2008).

### 3.2. Faulty data

The second case concerns data sets where a considerable amount of intensity is found on reciprocal space points that should have zero intensity according to the space-group symmetry. This can be due to the Renninger effect, overlap of systematically extinct reflections with non-extinct reflections of a minor twin component, or alternatively due to stacking or other structural faults. A first example is given by the data set of the organo-metallic complex flo2,  $C_{169}H_{152}B_8F_{32}Fe_4N_{25}O_{14}$ ,  $Z = 4$ , whose correct space group is  $P4_1$ , although this is overlooked by *XPREP* (Bruker, 1997) and *GRAL* (Oxford Diffraction, 2008). It should be noted that *PLATON*'s module *SPGRfromEx* does detect the  $4_1$  screw axis, but it is flagged as doubtful. Table 3 compiles the relevant statistics for this case and shows that the presence of the  $4_1$  screw axis is indeed doubtful, since  $\langle I/\sigma(I) \rangle = 9.55$  for the  $00l$ :  $l = 4n + 1$  reflections. The presence of an *ab*-glide perpendicular to the *a* axis seems more probable, based on  $\langle I/\sigma(I) \rangle = 7.41$  alone. The ratio of the mean intensity between reflections satisfying the reflection criterion and those not satisfying it (*t/f*), seems therefore a better indicator of the presence of a reflection condition, although even then it is not clear where to put the threshold for deciding whether the reflection condition exists or not. The  $b^a$ -glide is ranked second, with *t/f* = 4.90, just behind the  $4_1^c$  screw axis, with *t/f* = 8.20; it is not possible to argue whether the threshold should be placed at *t/f* = 5.0 or another value. *SUPERFLIP* solves this structure of 1008 non-H atoms in the  $P1$  unit cell in 277 iterations using data merged according to  $4/m$  Laue symmetry and keeping all reflections. The presence of the  $4_1^c$  and  $2_1^c$  screw axes shows up very clearly from the symmetry analysis of the resulting electron density map, the agreement factors showing a large gap between the

symmetry operations present and those that are absent in the electron density map.

It is interesting to note that the presence of the  $4_1^+$  screw axis would have been immediately obvious by looking at a simulated precession image of the  $a^*c^*$  plane. Fig. 1 shows the  $h0l$  reciprocal plane reconstructed from the data collection frames; the first space-group choice for structure solution using direct methods would be  $P4_1$ . A detailed description of the structure will be published elsewhere (Dimutru *et al.*, 2008).

The data set of structure **2** of Legrand *et al.* (2008) ( $C_{14}H_{17}N_5O$ ,  $a = 9.39$ ,  $b = 11.44$ ,  $c = 27.42$  Å,  $\alpha = 90$ ,  $\beta = 90$ ,  $\gamma = 90^\circ$ ,  $V = 2944.6$  Å<sup>3</sup>) presents a similar case, the true space group being  $Pcab$  (before transformation), but the reflection condition corresponding to the  $c^a$ -glide, *i.e.*  $0kl$ :  $l = 2n + 1$ , being polluted by spurious intensity, giving a fairly large value for  $\langle I/\sigma(I) \rangle$  (6.8). Again, *PLATON* sorts out the correct space group but it is flagged as doubtful, whereas *XPREP* does not give any proposition, and *GRAL* gives an incorrect space group,  $Pmab$ . The structure solution by *SUPERFLIP* runs smoothly and the correct space group is proposed without any ambiguity, with the seven nontrivial symmetry operations having agreement factors  $\phi_{\text{sym}}$  between 0.03 and 0.12 and all other symmetry operations compatible with the lattice having values of higher than 0.68.

### 3.3. Centrosymmetric/noncentrosymmetric ambiguity

In many cases there is no doubt about the correctness of the extinction conditions, but a choice has to be made between a centrosymmetric and a noncentrosymmetric space group.

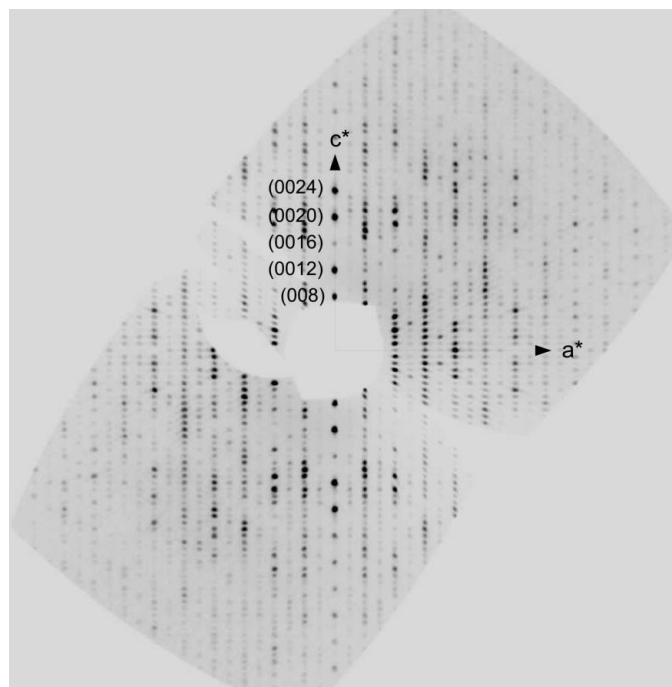


**Figure 1**  
Reconstructed  $h0l$  reciprocal plane for data set flo2, showing clearly the presence of a  $4_1$  screw axis.

Additional physical tests can be performed to ascertain whether the inversion center is present or not, and also a calculation of the mean value of  $|E^2 - 1|$  can be helpful, where  $E$  is a normalized structure-factor amplitude. For noncentrosymmetric structures the theoretical value is 0.736, whereas for centrosymmetric structures it is 0.968. Alternatively, the complete experimental probability distribution of normalized amplitudes can be compared with the theoretical ones, which show marked differences, or the intensities of Friedel-related reflection differences can be compared. The use of statistical values is, however, not always reliable (Hargreaves, 1955; Marsh, 1981).

For organic molecules and metallo-organic complexes a simple count of the expected non-H atoms compared with the volume of the unit cell can be helpful to distinguish the centrosymmetric and noncentrosymmetric space groups, as long as the molecules are not on symmetry elements. For inorganic compounds this is less useful, since very often the chemical formula is known only approximately, if at all.

We present here two cases: a trivial one for an inorganic compound with an uncertain starting composition, and a metallo-organic complex with  $\langle |E^2 - 1| \rangle = 0.904$ ,  $\langle |E^2 - 1|^2 \rangle = 2.15$  and  $\langle |E^2 - 1|^3 \rangle = 14.75$  all clearly in favor of a centrosymmetric space group, whereas the correct space group is noncentrosymmetric.

The inorganic compound,  $K_3Ga_2(PO_4)_3$  (Beurain *et al.*, 2008), was synthesized from 85 wt%  $K_2MoO_4$  and 15 wt%  $\alpha$ - $GaPO_4$  by a flux method; the resulting stoichiometry and even the elements in the final phase cannot be easily guessed. The extinction conditions point to either  $P2_1nb$  or  $Pmnb$  as possible space-group symmetries. The value of  $|E^2 - 1|$  is 0.752, leaving not much doubt about the absence of the center of inversion. All space-group determination programs select the correct space group. The analysis of the electron density map obtained by *SUPERFLIP* yielded symmetry agreement factors 0.10, 0.03 and 0.07 for the  $2_1^+$  screw axis, the  $n^b$ -glide and the  $b^c$ -glide, respectively, and 0.37 and 0.45 for the  $m^a$  mirror plane and the inversion center, respectively. The map interpretation was performed by *EDMA* (van Smaalen *et al.*, 2003) using the 'unknown stoichiometry' option with possible element types Ga, K, P and O; out of the two Ga atoms, three K atoms, three P atoms and 12 O atoms in the asymmetric unit only one O atom was missed.

The second compound,  $C_8H_{12}ClCuN_4O_4$ ,  $Z = 12$ , was described by Csöregi *et al.* (1975) in the noncentrosymmetric space group  $Pna2_1$ . We happened to synthesize the same compound and used these data for the present analysis. The space-group determination modules of *GRAL* and *XPREP* propose  $Pnam$  as the correct space group, probably because the  $E$  statistics are in favor of a centrosymmetric space group, whereas *PLATON* suggests  $Pnaa$ , with  $Pna2_1$  as a second choice. Analysis of the *SUPERFLIP* electron density map gives symmetry agreement factors of 0.05, 0.04 and 0.08 for the  $n^a$ -glide, the  $a^b$ -glide and the  $2_1^+$  screw axis, respectively. The  $a^c$ -glide is clearly absent, with an agreement factor of only 0.49. All other non-matching symmetry elements have agreement factors higher than 0.47 (0.52 for the inversion

center). The structure turns out to be an inversion twin with Flack parameter 0.405 (11).

### 3.4. Extinctionless cases

There are a number of cases in which the extinction symbol is  $---$  and which correspond to several probable space groups. The case that will be discussed here is that for a primitive tetragonal crystal system with Laue symmetry  $4/m$ . When there are no systematic extinctions the possible space groups are  $P4$ ,  $P\bar{4}$  and  $P4/m$ . The distinction between these space groups can only be made on the basis of non-diffraction methods, *i.e.* they are chiral, noncentrosymmetric and centrosymmetric, respectively. Nowadays space-group determination routines make the distinction in these cases usually on the basis of the value  $\langle |E^2 - 1| \rangle$  and of the space group frequency found in the CSD or ICSD; they will favor therefore  $P\bar{4}$  when  $\langle |E^2 - 1| \rangle$  tends to the noncentrosymmetric theoretical value, since its occurrence is an order of magnitude higher than that of  $P4$ .

In order to illustrate the problem we give here the determination of the space group of CSD refcode FOYTAA01 (Bolte, 2008),  $C_{12}H_{20}O_6$ ,  $Z = 8$ , with reported space group  $P4$ .  $\langle |E^2 - 1| \rangle = 0.823$  for the present data set, favoring slightly the two noncentrosymmetric space groups. All three space-group determination modules used in this study select  $P\bar{4}$  as the most probable space group, based mainly on the much higher occurrence of  $P\bar{4}$  than that of  $P4$  and  $P4/m$  in the databases. *SUPERFLIP* solves the structure smoothly and gives final symmetry agreement factors of 0.069, 0.848 and 0.523 for the presence of the  $4^c$  axis, the  $\bar{4}^c$  axis and the inversion center, respectively, which does not leave any doubt about the correct space group.

### 3.5. Missing reflection classes

It may happen that certain reflection classes that are necessary for a space-group determination based on systematic extinctions are missing, because the crystal is mounted along a crystal axis, creating a blind region. This may be cured easily, of course, by mounting the crystal differently or measuring a second differently mounted crystal. It is shown in this section that the absence of one axial reflection row is not a serious problem for space-group determination if the algorithm of this study is used. We used the data deposited at the PDB with code 1mfm, for which the reported space group is  $P2_12_12_1$ ,  $a = 34.99$ ,  $b = 48.11$ ,  $c = 81.08$  Å (Ferraroni *et al.*, 1999). If all  $00l$  reflections were missing then there would be an ambiguity between space group  $P2_12_12_1$  and  $P2_12_12$ , since no testing of the presence or absence of the  $2_1^c$  screw axis can be performed. Knowing that the space-group frequency of  $P2_12_12_1$  is about four times higher than that of  $P2_12_12$  (in the PDB), the logical first choice would be to test  $P2_12_12_1$ , but the chance that this is not the correct space group is relatively high. Using the symmetry-determination routine implemented in *SUPERFLIP* the question is not important, since the structure is solved in  $P1$ . All  $00l$  reflections were deleted from the deposited data and *SUPERFLIP* solved the structure

**Table 4**

Agreement factors for symmetry operations of the space group  $P4_12_12$  in the low-temperature structure of 4-methylpyridine-*N*-oxide.

The column 'Charge flipping' contains the range of agreement factors obtained from ten structure-solution attempts using charge flipping with histogram matching. The column 'Published structure' contains agreement factors obtained from the electron density generated from the published structure with declared space group  $P4_1$ .

Symmetry operation	Charge flipping	Published structure
$4_1^c$	0.03–0.05	0.00
$4_3^c$	0.03–0.05	0.00
$2_1^c$	0.05–0.09	0.00
$2^{a+b}$	0.17–0.25	0.05
$2^{a-b}$	0.14–0.22	0.05
$2_1^a$	0.15–0.23	0.05
$2_1^b$	0.16–0.24	0.05

using default parameters for protein-sized structures in about 3500 iterations. The correct space group  $P2_12_12_1$  was proposed with  $\phi_{\text{sym}}$  values for the three screw axes below 0.20 and for all other possible symmetry operations above 0.85.

### 3.6. Powder data

The ambiguity in symmetry determination from powder data is much more serious than that from single-crystal data. This is especially true for structures with symmetry higher than orthorhombic, where it is impossible to distinguish different Laue classes within one crystal system. The systematic absences are also often obscured by systematic as well as random reflection overlap. An illustrative example is the low-temperature structure of 4-methylpyridine-*N*-oxide. The structure was originally solved by simulated annealing, starting from the known structure of the room-temperature phase (Damay *et al.*, 2006). The authors performed a search of subgroups of the room-temperature space group  $I4_1/amd$  compatible with the observed cell doubling along two cell axes and concluded that the only convergent solution was obtained in  $P4_1$ .

The structure was solved *ab initio* using charge flipping combined with histogram matching (Baerlocher *et al.*, 2007) and the published solution could be confirmed. We decided to use the new symmetry-determination method to check the symmetry of the structure. Surprisingly, the symmetry analysis revealed that the structure has most probably the space group  $P4_12_12$  with agreement factors of individual symmetry operations given in Table 4. Inspection of the table shows that the  $4_1$  axis has systematically lower agreement factors than the perpendicular twofold axes and screw axes. This might suggest a pseudosymmetry rather than true symmetry elements. However, one should bear in mind that the histogram matching procedure uses the expected Laue group to average intensities of the symmetry-related reflections, and thus pairs of equivalent reflections in the space group  $P4_12_12$  were treated as independent in the procedure. This effect is likely to make the symmetry fit less perfect. To further test the hypothesis about the higher symmetry, the same symmetry analysis was applied to an electron density generated from the published structure. The density was obtained by Fourier

summation of calculated structure factors with  $\sin \theta/\lambda \leq 0.6$ . The resulting agreement factors are also listed in Table 4 and confirm that the higher symmetry is present even in the published structure, and it is thus not an artifact of the structure solution by charge flipping. The higher symmetry was then confirmed by structure refinement. A full structure report in the correct symmetry will be published elsewhere (Damay *et al.*, 2008).

### 3.7. Incommensurate structure

PbBi<sub>2</sub>VO<sub>6</sub> forms an incommensurately modulated phase that can be described in the superspace group  $P2_1/m(0\beta 0)s0$  (Roussel *et al.*, 2008). The symmetry  $P2_1/m$  of the average structure together with the modulation vector  $\mathbf{q} = (0, 0.23, 0)$  lead to two possible superspace groups:  $P2_1/m(0\beta 0)s0$  and  $P2_1/m(0\beta 0)00$ . These two superspace groups differ in the extinction condition for the reflection class  $0k0m$ . The former corresponds to a condition  $0k0m: k + m = 2n$  and the latter to  $0k0m: k = 2n$ . The two space groups can thus be distinguished only from the intensity distribution of the satellites. In the diffraction experiment only satellite reflections with  $m \leq 2$  were observed. A detailed inspection of the diffraction data shows that no satellite with significant intensity violates the first reflection condition, and only one satellite with  $I/\sigma(I) = 3.48$  violates the second condition. Obviously, it is not possible to distinguish these two space groups based on the reflection intensities alone.

The structure can be solved easily by *SUPERFLIP*. The symmetry-determination algorithm proposes the correct superspace group  $P2_1/m(0\beta 0)s0$ . The symmetry agreement factors leave no doubt about the superspace group, with  $\phi_{\text{sym}}$  of the correct symmetry operation ( $2_1|s$ ) equal to 0.12 and  $\phi_{\text{sym}}$  of the incorrect ( $2_1|0$ ) equal to 0.54.

### 3.8. Pseudosymmetry – a word of caution

The preceding examples represent cases where the new symmetry determination algorithm performs better than the traditional ones and where it gives the correct answer. However, even the new algorithm can sometimes fail in the automatic determination of the space group. It was described in §2.5 that a symmetry operation is included in the list of space-group elements if  $\phi_{\text{sym}}$  is lower than a given threshold, in the present case 0.25. Occasionally, however, a significant part of the structure exhibits a higher symmetry than the rest of the structure. This can be the case, for example, in organo-metallic complexes, where the heavy atoms often respect a higher symmetry than the organic ligands. If the pseudosymmetry is strong,  $\phi_{\text{sym}}$  of the pseudosymmetry elements can be quite low. In such a case the automatic space-group determination will result in a choice of a higher symmetry, often accompanied by an apparent disorder of one or more functional groups. It is up to the crystallographer to decide whether the disordered model in the higher-symmetrical group is to be preferred or if an ordered model in a lower-symmetrical space group should be accepted with possibly twice as many refineable para-

meters. In many cases the high-symmetry space group should be preferred (Marsh, 1986).

A careful inspection of the  $\phi_{\text{sym}}$  factors for the possible space-group operations may reveal these problems before the refinement, especially in the case of high-quality data. Ng (2005) re-refined the structure of a polymeric organo-metallic complex,  $\{[\text{Co}(\text{C}_4\text{H}_4\text{N}_2)(\text{H}_2\text{O})_4](\text{C}_8\text{H}_4\text{O}_4)\}_n$ , in the noncentrosymmetric space group *Imm2* using a fully ordered model, whereas it was originally refined using a disordered model yielding a relatively high residual index (Yang *et al.*, 2003) in the centrosymmetric space group *Immm*. Processing of the deposited observed structure factors by *SUPERFLIP* gives  $\phi_{\text{sym}}$  factors of 0.01, 0.04 and 0.13 for  $m^a$ ,  $m^b$  and  $m^c$ , respectively. The  $2^a$ ,  $2^b$  and  $2^c$  rotation axes have  $\phi_{\text{sym}}$  equal to 0.17, 0.14 and 0.05, respectively. The inversion center gives  $\phi_{\text{sym}} = 0.18$ . The  $\phi_{\text{sym}}$  parameters of the symmetry operations of *Imm2* are consistently about three times lower than  $\phi_{\text{sym}}$  of the remaining symmetry operations of *Immm*, and thus *Imm2* comes out as the best candidate. However, since the  $\phi_{\text{sym}}$  values of all symmetry operations of *Immm* are below 0.25, *SUPERFLIP* will propose in automatic mode *Immm* as the best space group.

Another example is given by the refinement of  $[\text{Cu}(\text{C}_3\text{H}_5\text{N}-\text{O}_5\text{S})(\text{C}_{10}\text{H}_8\text{N}_2)(\text{H}_2\text{O})] \cdot 2\text{H}_2\text{O}$  by Li *et al.* (2007), presented in *P1* with two independent mononuclear complex molecules and four uncoordinated water molecules in the unit cell (and thus in the asymmetric unit). Although not referred to in the text, the two molecules are nearly related to each other by an inversion center. The *SUPERFLIP* run using the deposited observed structure factor amplitudes indicates  $\phi_{\text{sym}}(\bar{1}) = 0.17$ , leaving indeed some doubts about the presence or absence of the inversion center. Again, on the basis of the cut-off of 0.25, *SUPERFLIP* would propose  $P\bar{1}$  as the most likely space group, which leads to a partially disordered structural model with a relatively high residual agreement factor.

With high-quality data intermediate  $\phi_{\text{sym}}$  values between 0.10 and 0.25 indicate potentially pseudosymmetric elements, which thus may or may not be considered for determining the space group and performing the refinement. The least *SUPERFLIP* does is to quantify the presence of these elements; it is up to the crystallographer to decide about the best space group.

Obviously, the problem of pseudosymmetry is not unique to the presented method but affects also other symmetry-determination and structure-solution methods. However, if the pseudosymmetric symmetry operation is a nonsymmorphic one, it can happen that  $\phi_{\text{sym}}$  is low, but the deviation from the perfect symmetry is sufficient to observably violate the extinction conditions. Therefore it is advisable to pay increased attention if the refined structure exhibits disorder and if the space group derived using the symmetry agreement factors corresponds to a different extinction symbol from that derived directly from the integrated intensities.

## 4. Discussion

It should be emphasized that the presented method is not merely an alternative to the established symmetry determi-

nation methods. What we suggest is a change of paradigm: if the structure solution in *P1* is equally feasible or even easier than the solution in the correct space group, then it is natural that the determination of the symmetry follows the structure solution rather than preceding it, removing thus one source of ambiguity in the structure-solution process. Determination of symmetry after the structure solution rather than before is a much easier task. The difference is demonstrated on several examples where space-group determination using the classical methods is not possible or at least doubtful; the new symmetry-finding routine presented in this paper is able to make a clear distinction for these cases between symmetry operations that are present in the structure and those which are not.

It should also be mentioned that the space-group determination modules of contemporary crystallographic programs perform well enough to select the correct space group in a large majority of cases. In this study we highlighted cases that could be problematic when the modules are used as black boxes, but which probably would have been solved by most experienced crystallographers after manual intervention. However, an ambiguity in the space-group determination is nowadays a bottleneck in an automated structure-solution process, and we believe that the presented approach is an important step towards more reliable and more straightforward structure solutions.

The computational efforts per trial to solve a structure scale roughly with the number of independent atoms to be determined, giving in general a faster structure solution if symmetry is employed than if it is not, at the condition that the number of trials needed to solve the structure is identical. Interestingly the number of trials is often lower when the structure is solved in *P1* than when symmetry is employed, thus giving, especially for large structures, an advantage in total computational time (Burla *et al.*, 2000). The (mandatory) symmetry search *after* the structure-solution step in *P1* – being only marginal in computational effort compared with the solution step – reinforces this advantage, since a wrong space-group decision before the solution attempt will prevent the solution completely, giving for large structures an important lengthening of the time needed to solve the structure.

It is interesting to compare *SUPERFLIP*'s symmetry-finding routine with the *ADDSYM* module in *PLATON*, which aims at finding missed higher crystallographic symmetry in a refined structure and is based on the original *MISSYM* algorithm (LePage, 1987, 1988). *ADDSYM* was used to recover the full space-group symmetry from the atom list found by *EDMA* by analysis of the electron density map of *SUPERFLIP* in *P1*. For flo2, *ADDSYM* is not able to propose the correct space group, whereas for flo19 the correct one is proposed. It may not be surprising that *ADDSYM* is somewhat less successful than the symmetry-finding routine in *SUPERFLIP* at finding the correct space-group symmetry, since *ADDSYM* works on refined atom lists, which supposes that the imposed atomic model is – apart from some symmetry elements – reasonably correct. The atom list found by *EDMA* may still contain some errors or omissions and is not yet

refined. *SUPERFLIP* finds symmetry elements in an atom-less mode, based on scattering density only.

Alternatively, *SUPERFLIP* may be used to find missed higher crystallographic symmetry in refined structures. We analyzed the nine structures in the C category of the paper of Marsh *et al.* (2002), where the missing symmetry is a result of overlooked systematic absences. The original CIF files were used to generate electron density maps, which were subsequently analyzed by the symmetry-finding algorithm of *SUPERFLIP*. The correct space group was found in all cases.

## 5. Conclusion

We have proposed a space-group determination algorithm based on an analysis of the scattering density solved in *P1*. We demonstrate the advantages of this approach on several examples from various fields of crystal-structure determination. In the presented approach the symmetry is determined after, and not before, the structure solution, thus eliminating the need for the determination of the space groups only from the diffracted intensities. We believe that, with the advent of methods solving routinely crystal structures in *P1*, the presented symmetry-determination method has the potential to become a standard practice for routine structure solution.

The authors are grateful to Dr M. Barboiu (Montpellier) and P. Roussel (Lille) for permitting the use of the diffraction data for this methodological study prior to publication of the structure–chemical results. We thank also V. Petříček (Prague) for pointing us to the example of the incommensurate structure. F. Dimutru and Y.-M. Legrand (Montpellier) are thanked for growing the crystals used for the data collections. M. Bolte (Frankfurt) is thanked for providing the unmerged data set of the structure in space group *P4*. This work was supported by the Swiss National Science Foundation, grant No. 20-105325.

## References

- Altomare, A., Caliandro, R., Camalli, M., Cuocci, C., da Silva, I., Giovacazzo, C., Moliterni, A. G. G. & Spagna, R. (2004). *J. Appl. Cryst.* **37**, 957–966.
- Baerlocher, C., McCusker, L. & Palatinus, L. (2007). *Z. Kristallogr.* **222**, 47–53.
- Beaurain, M., Astier, R., Lee, A. van der & Armand, P. (2008). *Acta Cryst.* **C64**, i5–i8.
- Bolte, M. (2008). Private communication.
- Bruker (1997). *XPREP*. Version 5.1. Bruker AXS Inc., Madison, Wisconsin, USA.
- Burla, M. C., Caliandro, R., Camalli, M., Carrozzini, B., Cascarano, G. L., De Caro, L., Giovacazzo, C., Polidori, G. & Spagna, R. (2005). *J. Appl. Cryst.* **38**, 381–388.
- Burla, M. C., Carrozzini, B., Cascarano, G. L., Giovacazzo, C. & Polidori, G. (2000). *J. Appl. Cryst.* **33**, 307–311.
- Csöregi, I., Kierkegaard, P. & Norrestam, R. (1975). *Acta Cryst.* **B31**, 314–317.
- Damay, F., Carretero-Genevri, A., Cousson, A., Van Beeck, W., Rodriguez-Carvajal, J. & Fillaux, F. (2006). *Acta Cryst.* **B62**, 627–633.
- Damay, F., Cousson, A., Rodriguez-Carvajal, J. & Palatinus, L. (2008). In preparation.
- Dimutru, F., Legrand, Y.-M., van der Lee, A. & Barboiu, M. (2008). In preparation.

- Elser, V. (2003). *Acta Cryst.* **A59**, 201–209.
- Ferraroni, M., Rypniewski, W., Wilson, K. S., Viezzoli, M. S., Banci, L., Bertini, I. & Mangani, S. (1999). *J. Mol. Biol.* **288**, 413–426.
- Hahn, T. (2002). Editor. *International Tables for Crystallography*, Vol. A, 5th ed. Dordrecht: Kluwer Academic Publishers.
- Hargreaves, A. (1955). *Acta Cryst.* **8**, 12–14.
- Hendrixson, T. & Jacobson, R. (1997). *Z. Kristallogr.* **212**, 577–585.
- Legrand, Y.-M., Michau, M., van der Lee, A. & Barboiu, M. (2008). *CrystEngComm*, **10**, 490–492.
- Le Page, Y. (1987). *J. Appl. Cryst.* **20**, 264–269.
- Le Page, Y. (1988). *J. Appl. Cryst.* **21**, 983–984.
- Li, H.-Y., Huang, F.-P., Jiang, Y.-M. & Ng, S. W. (2007). *Acta Cryst.* **E63**, m219–m220.
- Markvardsen, A. J., David, W. I. F., Johnson, J. C. & Shankland, K. (2001). *Acta Cryst.* **A57**, 47–54.
- Marsh, R. E. (1981). *Acta Cryst.* **B37**, 1985–1988.
- Marsh, R. E. (1986). *Acta Cryst.* **B42**, 193–198.
- Marsh, R. E., Kapon, M., Hu, S. & Herbstein, F. H. (2002). *Acta Cryst.* **B58**, 62–77.
- Ng, S. W. (2005). *Acta Cryst.* **E61**, m2297–m2298.
- Oszlányi, G. & Sütő, A. (2004). *Acta Cryst.* **A60**, 134–141.
- Oszlányi, G. & Sütő, A. (2007). *Acta Cryst.* **A63**, 156–163.
- Oszlányi, G. & Sütő, A. (2008). *Acta Cryst.* **A64**, 123–134.
- Oxford Diffraction (2008). *GRAL*. Oxford Diffraction Ltd, Abingdon, Oxfordshire, UK.
- Palatinus, L. (2004). *Acta Cryst.* **A60**, 604–610.
- Palatinus, L. & Chapuis, G. (2007). *J. Appl. Cryst.* **40**, 786–790.
- Petříček, V., Dušek, M. & Palatinus, L. (2006). *JANA2006*. Institute of Physics, Prague, Czech Republic.
- Roussel, P., Labidi, O., Huv, M., Drache, M., Wignacourt, J. & Petříček, V. (2008). In preparation.
- Sheldrick, G. M. (2008). *Acta Cryst.* **A64**, 112–122.
- Sheldrick, G. M. & Gould, R. O. (1995). *Acta Cryst.* **B51**, 423–431.
- Smaalen, S. van, Palatinus, L. & Schneider, M. (2003). *Acta Cryst.* **A59**, 459–469.
- Spek, A. L. (2003). *J. Appl. Cryst.* **36**, 7–13.
- Yang, S.-Y., Long, L.-S., Huang, R.-B., Zheng, L.-S. & Ng, S. W. (2003). *Acta Cryst.* **E59**, m961–m963.